

---

## Evidence for efficient cosmic ray acceleration in SN 1006

---

E.G. Berezhko<sup>1</sup>, L.T. Ksenofontov<sup>1,2</sup> and H.J. Völk<sup>3</sup>

(1) *Institute of Cosmophysical Research and Aeronomy, 677891 Yakutsk, Russia*

(2) *Institute for Cosmic Ray Research, Univ. of Tokyo, Chiba 277-8582, Japan*

(3) *Max-Planck-Institut für Kernphysik, 69029 Heidelberg, Germany*

---

### Abstract

The nonlinear kinetic theory of cosmic ray (CR) acceleration in supernova remnants (SNRs) is used to describe the fine spatial structure of the nonthermal X-ray emission of the remnant of SN 1006, obtained in recent Chandra observations. The key property is the large interior magnetic field  $B_d \approx 100 \mu\text{G}$  which had been postulated earlier by the present authors in order to fit the spatially integrated radio and  $\gamma$ -ray synchrotron spectra and the overall morphological structure. Such a large effective field strength can only be produced by the efficiently accelerated nuclear CR component. It is concluded that the appropriate interpretation of the Chandra data is that they verify this large field, and that SN 1006 indeed accelerates nucleonic CRs with the high efficiency required for SNRs to be considered as the main Galactic CR sources.

### 1. Introduction

Nonthermal X-ray observations indicate that at least CR electrons are accelerated in several SNRs. SN 1006 is one of the objects for which there is evidence that electrons reach energies of about 100 TeV [1,2]. Also TeV  $\gamma$ -ray emission from this source has been reported [3].

The selfconsistent nonlinear kinetic theory of CR acceleration in SNRs [4,5], applied to SN 1006 [6], has demonstrated that the existing data require a high value  $B_d \approx 100 \mu\text{G}$  of the interior magnetic field strength and thus very efficient acceleration of CR nuclei at the SN shock wave which converts a significant fraction of the initial SNR energy content into CR energy. Nevertheless, the existing observations in the case of SN 1006 do not strongly exclude a solution in which nuclear CRs play no important role and all nonthermal emissions are of leptonic origin (inefficient solution). Therefore we have applied the detailed solutions of our theory to recently reported Chandra data on extremely small spatial scales of the nonthermal X-ray emission from SN 1006 [7].

## 2. Analytical estimates and numerical results

The distribution of CRs produced by the spherically expanding shock of radius  $R_s$  and speed  $V_s$  can be roughly described by the steady state one-dimensional transport equation for the CR distribution function  $f(r, p, t)$

$$\kappa \frac{\partial^2 f}{\partial x^2} - u \frac{\partial f}{\partial x} + \frac{p}{3} \frac{du}{dx} \frac{\partial f}{\partial p} - L = 0, \quad (1)$$

where  $x = R_s - r$ , and  $u = V_s - w$  is the speed of the scattering medium relative with respect to the shock front,  $w$  is the speed in the frame of the progenitor star,  $\kappa(p)$  is the CR diffusion coefficient,  $p$  is particle momentum,  $L$  is a loss term, which we take in the simple form  $L = f/\tau$ , where  $\tau$  is the loss time. Within this approach we neglect any effects of the shock modification due to the CR backreaction. Therefore the velocity profile has the form:  $u(x < 0) = u_1 = V_s$ ;  $u(x > 0) = u_2 = u_1/\sigma$ , where  $\sigma = 4$  is the shock compression ratio.

The solution of the transport equation is [8]

$$f_i = f_0(p) \exp(-|x|/l_i), \quad (2)$$

where  $f_0(p) = f(x = 0, p)$  is the CR distribution function at the shock front and the scale

$$l_i = \frac{2\kappa_i}{u_i} \left[ 1 - (-1)^i \sqrt{1 + \frac{4\kappa_i}{u_i^2 \tau_i}} \right]^{-1} \quad (3)$$

describes the spatial CR distribution in the upstream ( $i = 1$ ) and downstream ( $i = 2$ ) regions.

In the cases of practical interest  $\tau_i \gg \kappa_i/u_i^2$  for the extended momentum interval from the injection momentum  $p_{inj}$  up to the maximum momentum  $p_{max} \gg p_{inj}$ , and we have approximately  $l_1 = \kappa_1/[u_1(1 + \kappa_1/(u_1^2 \tau_1))]$ ;  $l_2 = \tau_2 u_2$ .

The CR distribution function at the shock front is determined by the expression

$$f_0 = A p^{-q} \exp \left[ - \int_{p_{inj}}^p dp \phi(p)/p \right], \quad (4)$$

where  $q = 3u_1/(u_1 - u_2)$ ;  $\phi = q[\kappa_1/(u_1^2 \tau_1) + \kappa_2/(u_1 u_2 \tau_2)]$ .

The losses produce two effects: they cut off the power law spectrum at  $p > p_{max}$ , where  $\phi(p_{max}) = 1$ , and they reduce the spatial scales  $l_i$ . This is essential in the cutoff region  $p \sim p_{max}$ .

In reality, a SNR has rather spherical than plane parallel symmetry. The corresponding terms in the transport equation can be written as two further loss terms with loss times  $\tau_1 = R_s/(2u_1)$  and  $\tau_2 \sim R_s/V_s$ . As a result, the upper proton momentum is determined by the relation  $\kappa_1(p_{max}) = R_s V_s/A$ , where the factor  $A$  is of the order of 10 [9].

In addition to the above mechanical effects, CR electrons suffer synchrotron losses with a time scale  $\tau = 9m_e^2c^2/(4r_0^2B^2p)$ , where  $m_e$  is the electron mass,  $r_0$  denotes the classical electron radius, and  $B$  is the magnetic field strength. This is the dominant loss effect for our discussion.

For low fields, where  $\tau$  is smaller than the age  $t$  of the system, synchrotron losses are not important, with spatial scales  $l_{1,2} \sim 0.1R_s$ . However, for high magnetic field, both the electron cutoff is low compared to that of the nuclear particles, and the electrons are confined to a very thin region around the shock,  $l_{1,2} \ll 0.1R_s$ , for  $\tau \ll t$ .

For the full nonlinear solution of the transport equation in spherical symmetry, assuming the Bohm limit for the diffusion coefficient, we can compute the radial dependence of the X-ray synchrotron emissivity  $q_\nu(r)$  in  $\text{erg}/(\text{cm}^3\text{s})$ . The emissivity peaks sharply at the shock with scales  $l_{1,2} < 10^{-2}R_s$ , in very good agreement with the analytical estimate that follows from Eq. (3).

*In projection* along the line of sight, this radial emissivity profile determines the remnant's surface brightness. For the X-ray energy interval  $\epsilon_1 < \epsilon_\nu < \epsilon_2$  it has the form

$$J_\nu(\rho) \propto \int_{\epsilon_1}^{\epsilon_2} d\epsilon_\nu \int dx q_\nu(\epsilon_\nu, r = \sqrt{\rho^2 + x^2}) \quad (5)$$

where  $\rho$  is now the distance between the center of the remnant and the line of sight. Due to the shock curvature, the surface brightness profile  $J_\nu(\rho)$  differs significantly from the emissivity profile  $q_\nu(r = \rho)$ . The calculated brightness profile for the X-ray energy interval between  $\epsilon_1 = 2$  keV,  $\epsilon_2 = 10$  keV is shown in Fig. 1. Despite the fact that, formally speaking, the emissivity profile  $q_\nu(r)$  has a zero upstream scale  $l_1 = 0$ , the brightness profile is characterized by an outer scale  $L_1 = 0.002R_s = 0.015$  pc which comes from the emission of the downstream region alone, and from the shock curvature. The inner brightness scale is  $L_2 \approx 7L_1 = 0.1$  pc.

The sharpest experimental X-ray brightness profile obtained by the Chandra observers [7] is shown in Fig. 1. One can see that the experimental values agree very well with our calculations. All other observed brightness profiles are significantly wider [7]. There are several reasons for a broadening of the observed profile, compared with the ideal case of a spherical shell. First of all, it is clear from the observations that the actual shock front deviates from a spherical form. The wavy shape of the shock front can be produced as the result of a small scale density inhomogeneity of the ambient interstellar medium. Any small scale distortion of the spherical emission shell leads to a broadening of the observed brightness profile.

Confirming evidence can also be gained from the thermal X-ray emission profiles. The so-called inefficient model has an artificially reduced rate of suprathermal protons and also a low downstream field strength  $B_d = 16 \mu\text{G}$  [6], while being consistent with the overall nonthermal X-ray emission spectrum.

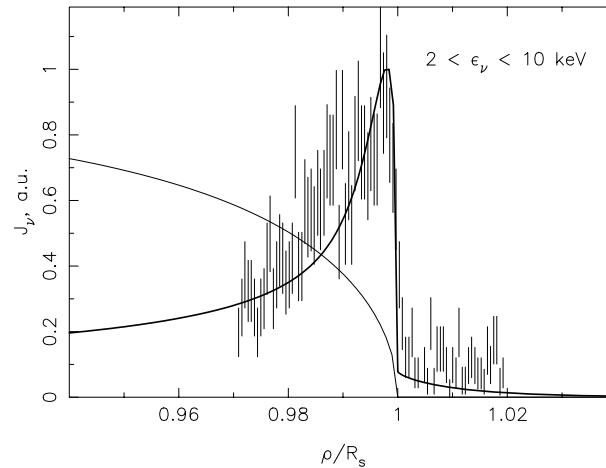


**Fig. 1.** Projected radial dependence of the X-ray brightness in the 2 to 10 keV X-ray energy interval. Thick and thin lines correspond to the efficient and inefficient model [6], respectively. The Chandra data, corresponding to the sharpest profile, are also shown [7].

Therefore it is clear that inefficient scenarios for nuclear CR injection/acceleration should be rejected, since they are in strong disagreement with the X-ray measurements. The strong field strength can only be created by Alfvén wave excitation due to the CR streaming instability, and if the CR pressure is comparable with the shock ram pressure, it becomes so efficient that it formally leads to a strong amplification of the large scale magnetic field [10].

This work has been supported in part by the Russian Foundation for Basic Research (grants 00-02-17728, 99-02-16325). EGB and LTK acknowledge the hospitality of the Max-Planck-Institut für Kernphysik, where part of this work was carried out. LTK also acknowledges the receipt of a JSPS Research Fellowship.

### 3. References

1. Koyama K., et al. 1995, *Nature* 378, 255
2. Allen, G.E., Petre, R. & Gotthelf, E.V. 2001, *ApJ* 558, 739
3. Tanimori, T., et al. 1998, *ApJ* 497, L25
4. Berezhko, E.G., Elshin, V.K. & Ksenofontov, L.T. 1996, *Sov. Phys. JETP* 82, 1
5. Berezhko, E.G. & Völk, H.J. 1997, *Astropart. Phys.* 7, 183
6. Berezhko, E.G., Ksenofontov, L.T. & Völk, H.J. 2002, *A&A* 395, 943
7. Bamba, A., et al. 2003, to appear in *ApJ*, (astro-ph/0302174)
8. Völk, H.J., Morfill, E.G. & Forman, M.A. 1981, *ApJ*, 249, 161
9. Berezhko, E.G. 1996, *Astropart. Phys.*, 5, 367
10. Lucek, S.G. & Bell, A.R. 2000, *MNRAS* 314, 65